Dynamic actin/septin network in megakaryocytes co-ordinates proplatelet elaboration

Isabelle C. Becker,[1,2*] Adrian R. Wilkie,[1,2*] Bret A. Unger,[3] Anthony R. Sciaudone,[4] Farheen Fatima,[1,2] I-Ting Tsai,[1,2] Ke Xu,[3] Kellie R. Machlus[1,2] and Joseph E. Italiano Jr[1,2]

[1]Vascular Biology Program, Boston Children's Hospital, Boston, MA; [2]Department of Surgery, Harvard Medical School, Boston, MA; [3]Department of Chemistry, University of California, Berkeley, CA and [4]Brigham and Women's Hospital, Boston, MA, USA

ICB and ARW contributed equally as first authors.

Correspondence: J. Italiano
joseph.italiano@childrens.harvard.edu

Received: April 19, 2023.
Accepted: August 18, 2023.
Early view: September 7, 2023.

https://doi.org/10.3324/haematol.2023.283369

Abstract

Megakaryocytes (MK) undergo extensive cytoskeletal rearrangements as they give rise to platelets. While cortical microtubule sliding has been implicated in proplatelet formation, the role of the actin cytoskeleton in proplatelet elongation is less understood. It is assumed that actin filament reorganization is important for platelet generation given that mouse models with mutations in actin-associated proteins exhibit thrombocytopenia. However, due to the essential role of the actin network during MK development, a differential understanding of the contribution of the actin cytoskeleton on proplatelet release is lacking. Here, we reveal that inhibition of actin polymerization impairs the formation of elaborate proplatelets by hampering proplatelet extension and bead formation along the proplatelet shaft, which was mostly independent of changes in cortical microtubule sliding. We identify Cdc42 and its downstream effectors, septins, as critical regulators of intracellular actin dynamics in MK, inhibition of which, similarly to inhibition of actin polymerization, impairs proplatelet movement and beading. Super-resolution microscopy revealed a differential association of distinctive septins with the actin and microtubule cytoskeleton, respectively, which was disrupted upon septin inhibition and diminished intracellular filamentous actin dynamics. *In vivo*, septins, similarly to F-actin, were subject to changes in expression upon enforcing proplatelet formation through prior platelet depletion. In summary, we demonstrate that a Cdc42/septin axis is not only important for MK maturation and polarization, but is further required for intracellular actin dynamics during proplatelet formation.

Introduction

Megakaryocytes (MK) are large, polyploid cells that primarily reside within the bone marrow. MK generate platelets by remodeling their cytoplasm into long proplatelet extensions, which extend through endothelial cells into the vascular lumen and serve as assembly lines for platelet production.[1] MK terminally differentiate from hematopoietic stem cells (HSC), and then mature in a complex process that culminates in polyploidization and an increase in cell size, including the development of a demarcation membrane system (DMS). Critically, both the significant assembly of cellular content as well as the ultimate production of platelets require extensive cytoskeletal rearrangements of both microtubules as well as filamentous (F)-actin structures. During proplatelet formation, MK penetrate the sinusoidal endothelium by forming transendothelial actomyosin-rich protrusions called podosomes that elongate into proplatelets within the vasculature.[2,3] Previous studies have identified that proplatelet formation *in vitro* is initiated in one pole, from which tubular structures with a shaft diameter of 2-4 μm emerge, elongate, and branch out.[4,5] Isolated proplatelets appear as strings with several platelet-sized beads lining the shaft and a proplatelet tip on each end.[5] Upon release, proplatelets can further mature into intermediate structures (termed preplatelets) and platelets both *in vitro* as well as in circulation.[5,6] Proplatelet shaft elongation is driven by microtubule sliding, while the motor proteins dynein and kinesin enable the simultaneous transport of granules along the developing proplatelets.[7,8] Post-translational modifications on both α-tubulins as well as on the MK-specific tubulin isoform β1 regulate proplatelet formation and motor protein movement within proplatelets.[9,10] In contrast to microtubules, the role of the actin cytoskeleton in proplatelet formation is much less understood. While transgenic mouse models lacking actin

regulatory proteins have markedly increased our understanding of the role of actin dynamics in MK,[11] determining how they regulate the final stages of proplatelet formation is hampered in murine models due to their unavoidable impact on the maturation of the DMS.[12,13]

Treatment of proplatelet-forming MK with the actin-depolymerizing agents cytochalasin D (CytoD) or latrunculin A (LatA) markedly reduces the number of proplatelet tips,[14,15] although an initial increase in proplatelet formation has paradoxically also been described.[16,17] These observations have led researchers to conclude that the F-actin cytoskeleton is important for increasing the number of existing proplatelet tips, but definite proof for this hypothesis is still lacking. One important pathway orchestrating actin dynamics during proplatelet formation involves the Rho GTPase Cdc42, one activator of the actin nucleation protein complex Arp2/3,[18] which is able to branch existing actin filaments through binding of nucleation promoting factors such as Wiskott-Aldrich protein (N-WASp) or WASp family verprolin homologous. However, while the percentage of proplatelet-forming MK derived from Arp2- or N-WASp-deficient mice *in vitro* is unaltered despite the microthrombocytopenia observed *in vivo*,[19,20] Cdc42-deficient MK display impaired proplatelet formation *in vitro*.[15,21] Inhibition of Cdc42 using the small molecule inhibitor CASIN impairs DMS polarization and proplatelet formation due to defective signaling of p21-activated kinases (PAK).[15,22] Of note, both Cdc42 and PAK are capable of activating another class of cytoskeletal proteins, namely septins.[23-25] The contribution of septins to megakaryo- and thrombopoiesis, however, has not yet been investigated.

Septins are a group of GTP-binding and scaffolding proteins, described as the fourth cytoskeletal component, that can assemble into filaments, rings, and gauzes. Thirteen septins have been described so far,[26] which can be divided into 4 different classes according to their sequence similarity: Sept2 (1, 2, 4 and 5), Sept6 (6, 8, 10, 11, 14), Sept7 and Sept9 (3, 9 and 12). While most are ubiquitously expressed, some exhibit cell type-specific expression, with Sept5 expression being highest in MK, platelets, and neurons.[27,28] Most septins (2, 4, 5, 6, 7, 8, 9 and 11) are expressed in human platelets; however, not all have been functionally studied.[29,30] Sept5 was the first platelet septin class to be characterized. It can associate with Sept4, 6, 7 and 9 and participates in granule secretion from platelets.[30,31] Sept2 and 9 co-localize with the microtubule cytoskeleton in human platelets, which can be inhibited through treatment with the universal septin inhibitor forchlorfenuron (FCF),[32] causing impaired clot retraction *in vitro*.[28] Mice lacking Sept8 exhibit unaltered platelet counts, but displayed impaired platelet activation and aggregation *in vitro*.[33] Although septins play important roles in regulating platelet function, their participation in cytoskeletal rearrangements in MK, including during proplatelet formation, has not yet been explored.

Here, we identify an intracellular F-actin network in MK that is essential for proplatelet beading and depends on interactions with septin proteins. These observations are reminiscent of a non-cortical F-actin network previously described in neurons,[34] in which F-actin dynamics are dependent on the function of formin homology domain proteins, actin nucleating factors that also play important roles in MK.[35] Our data provide a novel insight into how a third cytoskeletal component, the septin cytoskeleton, regulates actin dynamics, thus contributing to effective proplatelet formation.

Methods

Mice

CD-1 (#CD1(ICR)) and C57BL/6J mice (#027C57BL/6) were acquired from Charles River Laboratories (Worcester, MA, USA). All animal work was approved by the international animal care and use committee at Boston Children's Hospital, Boston, MA, USA (00001248).

Statistical analysis

Results are displayed as mean ± standard deviation (SD) from at least three independent biological replicates per group, or as otherwise indicated. Differences were statistically analyzed using unpaired, two-tailed Student *t* test, one- or two-way ANOVA with Sidak's correction for multiple comparisons. $P<0.05$ was considered statistically significant: *$P<0.05$; **$P<0.01$; ***$P<0.001$; ****$P<0.0001$. A detailed description of platelet depletion, MK isolation, proplatelet formation analysis and visualization, fluorescence recovery after photobleaching (FRAP), flow cytometry and three-dimensional stochastic optical reconstruction microscopy (3D-STORM) can be found in the *Online Supplementary Appendix*.

Results

Inhibition of actin polymerization decreases proplatelet beading and impairs movement

Although the role of microtubules during proplatelet elongation has been extensively studied, how the F-actin cytoskeleton contributes to this process is not well understood. To address this, we utilized a custom imaging pipeline to assess how actin depolymerization affected proplatelet formation from murine fetal liver-derived MK.[36] We confirmed that treatment with the actin polymerization inhibitors LatA or CytoD decreased proplatelet formation *in vitro* (Figure 1A).[15] However, proplatelet formation was initiated earlier upon both LatA and CytoD treatment, consistent with previous reports suggesting that actin inhibition might actually shorten the time course until platelet formation.[16] As visualized by confocal microscopy (Figure 1B), both the number of proplatelet elongations as well as the number

of beads per proplatelet shaft were significantly lower in LatA-treated samples (Figure 1C, D) suggesting that inhibition of actin polymerization hampered proplatelet beading. To visualize the underlying cytoskeletal defects in already formed proplatelets, we measured proplatelet movement in a static assay by quantifying changes in pixel location using live-cell imaging. While DMSO-treated proplatelets were highly motile and demonstrated characteristic extensions, LatA-treated proplatelets moved significantly less (Figure 1E, *Online Supplementary Videos S1, S2*). We verified these findings by assessing fluorescence positions in GFP-transduced MK over time in kymographs. DMSO-treated proplatelets showed diagonal lines indicative of movement, whereas cells treated with actin polymerization inhibitors exhibited vertical lines (Figure 1F). To investigate the physiological relevance of these findings, we utilized a proplatelet bioreactor previously established in our lab that broadly mimics shear conditions encountered *in vivo*.[37] We manually tracked the tips of proplatelets and plotted their position (Figure 1G) and mean velocity (Figure 1H) over time revealing that proplatelet tips extended at various different rates, with most proplatelet tips exhibiting periods of rapid extension and pausing (*Online Supplementary Video S3*).[7] In contrast, existing proplatelets treated with LatA for 30 minutes (mins) extended at a much slower rate (*Online Supplementary Video S4*) suggesting that actin polymerization enables proplatelet elongation and release under flow conditions.

Extensive studies have shown that inhibition of microtubule sliding prevents proplatelet elongation, suggesting that our observations upon inhibition of actin polymerization might solely be caused by defective microtubule sliding due to actin inhibition. To test this hypothesis, we visualized F-actin and α-tubulin in proplatelet-forming fetal liver-derived MK by immunofluorescence (Figure 1 I). While cortical microtubules were stable upon LatA treatment, the intracellular microtubule cytoskeleton appeared more dispersed. We next conducted FRAP imaging on released proplatelets isolated from MSCV-dendra2-β1-tubulin-transduced MK. While we observed significant recovery into bleached regions by calculating corrected fluorescence intensity in DMSO-treated proplatelets, the microtubule stabilizer taxol that prevents sliding abolished fluorescence recovery into bleached regions (Figure 1J, *Online Supplementary Videos S5, S6*).[7] In contrast, LatA-treated proplatelets exhibited a recovery only marginally slower than the control (*Online Supplementary Video S7*), thus demonstrating that defective proplatelet bead formation and motility occurred mostly independent of the cortical microtubule cytoskeleton. The existence of different actin networks has previously been observed in neurons, in which cortical (subplasmalemmal) F-actin fibers formed rings along axons,[38] while actin trails occurred intracellularly,[34] and long F-actin filaments extended along dendritic shafts. Whether cortical actin filaments exist and are regulated differently to intracellular fibers, however, has not been investigated in MK to date. To examine intracellular changes to the F-actin cytoskeleton during proplatelet extension, we transduced MK with MSCV-LifeAct-mRuby and observed highly dynamic changes manifesting as F-actin foci that emerged within proplatelet shafts (*Online Supplementary Video S8*). In summary, our data reveal that intracellular F-actin polymerization contributes to proplatelet bead formation and movement independent of the cortical microtubule cytoskeleton.

Inhibition of Cdc42/septins impairs megakaryocyte maturation and polarization

Our data revealed that intracellular F-actin was critical for efficient proplatelet generation; however, the molecular players regulating intracellular actin dynamics under steady state remained elusive. One molecular master-switch orchestrating actin dynamics in MK is the Rho GTPase Cdc42. F-actin-dependent polarization of the DMS is essential for the initiation of proplatelet formation and was previously shown to be affected by inhibition of Cdc42.[15,39] Moreover, PAK were identified as downstream effectors of Cdc42, inhibition or lack of which also impaired DMS development and subsequent proplatelet formation in a mouse model.[22] Among other proteins, PAK phosphorylate septins,[40] which prompted us to dissect whether septin inhibition during late MK maturation, similar to inhibition of Cdc42, would impair DMS polarization. Bone marrow-derived hematopoietic stem and progenitor cells (HSPC) were matured into MK using thrombopoietin (TPO) for 3 days upon which they were treated with the Cdc42 inhibitor CASIN or the universal septin inhibitor FCF for 24 hours (hrs). In line with previous studies,[15,41] MK were stained for F-actin and glycoprotein (GP)IX, which localizes to the DMS, imaged by confocal microscopy and divided into groups according to DMS morphology: MK with a single DMS invagination (stage I), MK with several invaginations and DMS territories (stage II), and MK with a clearly polarized DMS cap associated with F-actin fibers (stage III) (Figure 2A). Treatment of MK with both CASIN or FCF resulted in an increased percentage of MK in stage I, while stage III-MK were less abundant (Figure 2B, C), suggesting that both Cdc42 and septins are essential for the polarization of the DMS *in vitro*.

As mentioned above, Cdc42 was previously shown to be essential for the development of the DMS during MK maturation,[15,39] while the role of septins during this process has not been assessed before. To investigate this, we treated bone marrow-derived HSPC with different doses of CASIN or FCF, matured them into MK and assessed the percentage of CD41/CD42d-positive cells and the mean fluorescence intensity (MFI) of CD41 by flow cytometry. As expected, we found a reduced amount of double-positive mature MK upon treatment with 10 μM of CASIN (Figure 2A) as well as a reduced expression of CD41 (Figure 2B). Similarly, treatment of HSPC with the septin inhibitor FCF impaired MK maturation as assessed by CD41/CD42d-positivity (Figure

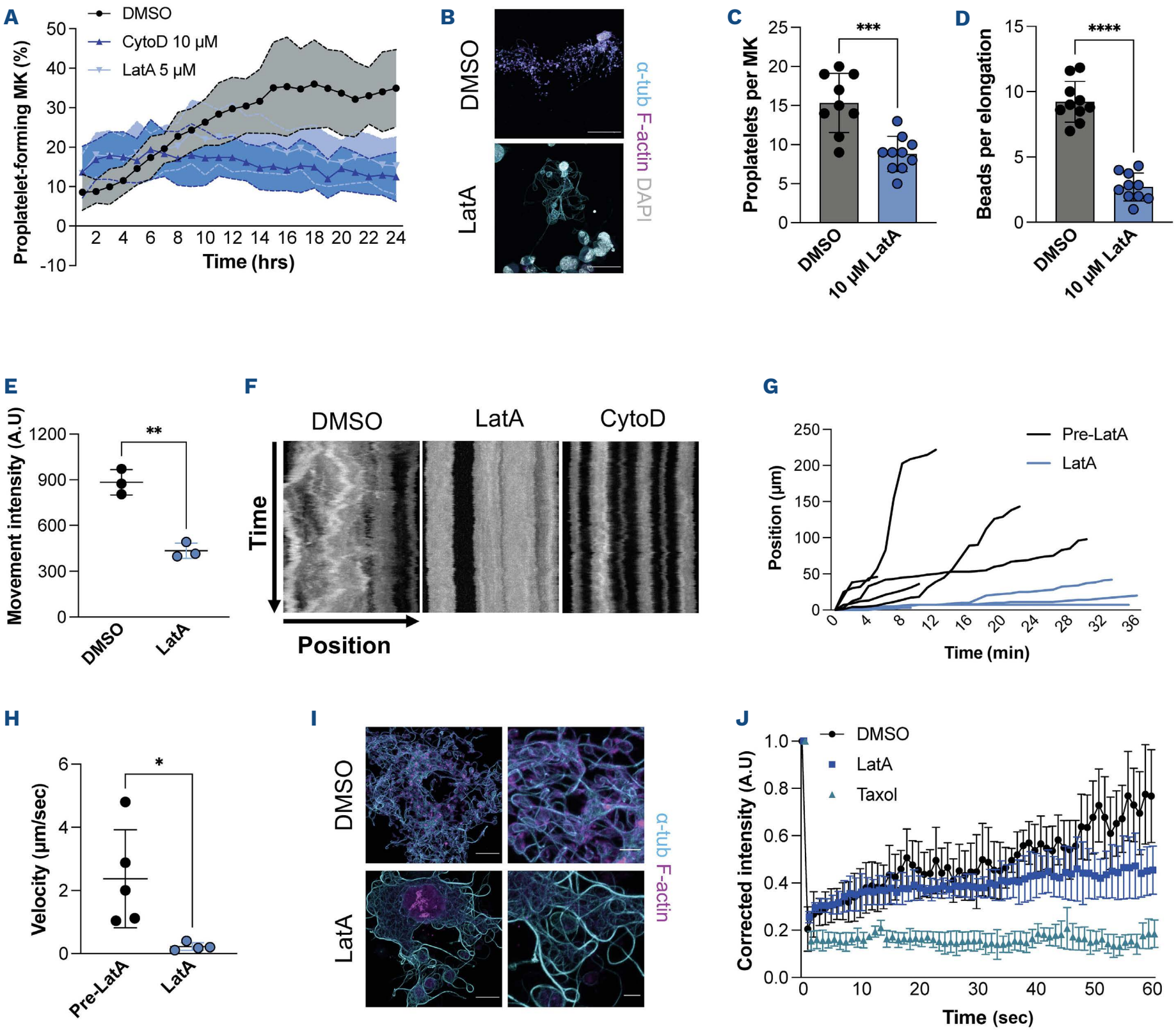

Figure 1. Inhibition of actin polymerization impairs proplatelet beading. (A) Fetal liver-derived megakaryocytes (MK) were treated with the indicated concentration of latrunculin A (LatA) and cytochalasin D (CytoD) or vehicle control (DMSO), and imaged every hour for 24 hours (hrs) using an Incucyte imaging system. Image analysis was performed using a custom image analysis pipeline as previously described.[36] (B) Immunofluorescence stainings for filamentous (F)-actin and α-tubulin in fetal liver-derived MK. Scale bars: 50 µm. (C and D) Quantification of proplatelets per MK (C) and beads per proplatelet shaft (D). Data presented as mean ± standard deviation (SD). One dot represents one cell. N=3. Unpaired, two-tailed Student *t* test. (E) Methylcellulose-embedded proplatelets were imaged using an automated imaging system. Analysis of proplatelet movement was conducted using Difference Tracker in ImageJ Software. N=3. Unpaired, two-tailed Student *t* test. (F) Isolated proplatelets of MSCV-GFP-transduced MK were imaged and analyzed by monitoring changes in fluorescence localization over a 4-hr time course with kymographs. (G and H) Analysis of proplatelet tip positions (G) and mean proplatelet tip velocities (H) pre- and post-LatA treatment of fetal liver-derived MK in a custom microfluidic device was performed using ImageJ (Manual Tracker).[37] Data presented as mean ± SD. Unpaired, two-tailed Student *t* test. (I) F-actin and α-tubulin were visualized using confocal microscopy in proplatelet-forming MK treated with DMSO or 10 µM LatA. Scale bars: 25 µm; insets: 5 µm. (J) Corrected intensity for each timepoint of fluorescence recovery after photobleaching (FRAP) on proplatelets derived from MSCV-β1-tubulin-dendra2-transduced fetal liver-derived MK treated with DMSO, 10 µM taxol, or 10 µM LatA. Data presented as mean ± SD of 5 individual cells. **P*<0.05; ***P*<0.01; ****P*<0.001; *****P*<0.0001. Min: minutes; secs: seconds.

2C) and CD41 MFI (Figure 2D), thus revealing a novel and significant role for septins in MK development. In summary, these findings point towards an essential role of Cdc42/septins in early and late stages of MK maturation *in vitro*.

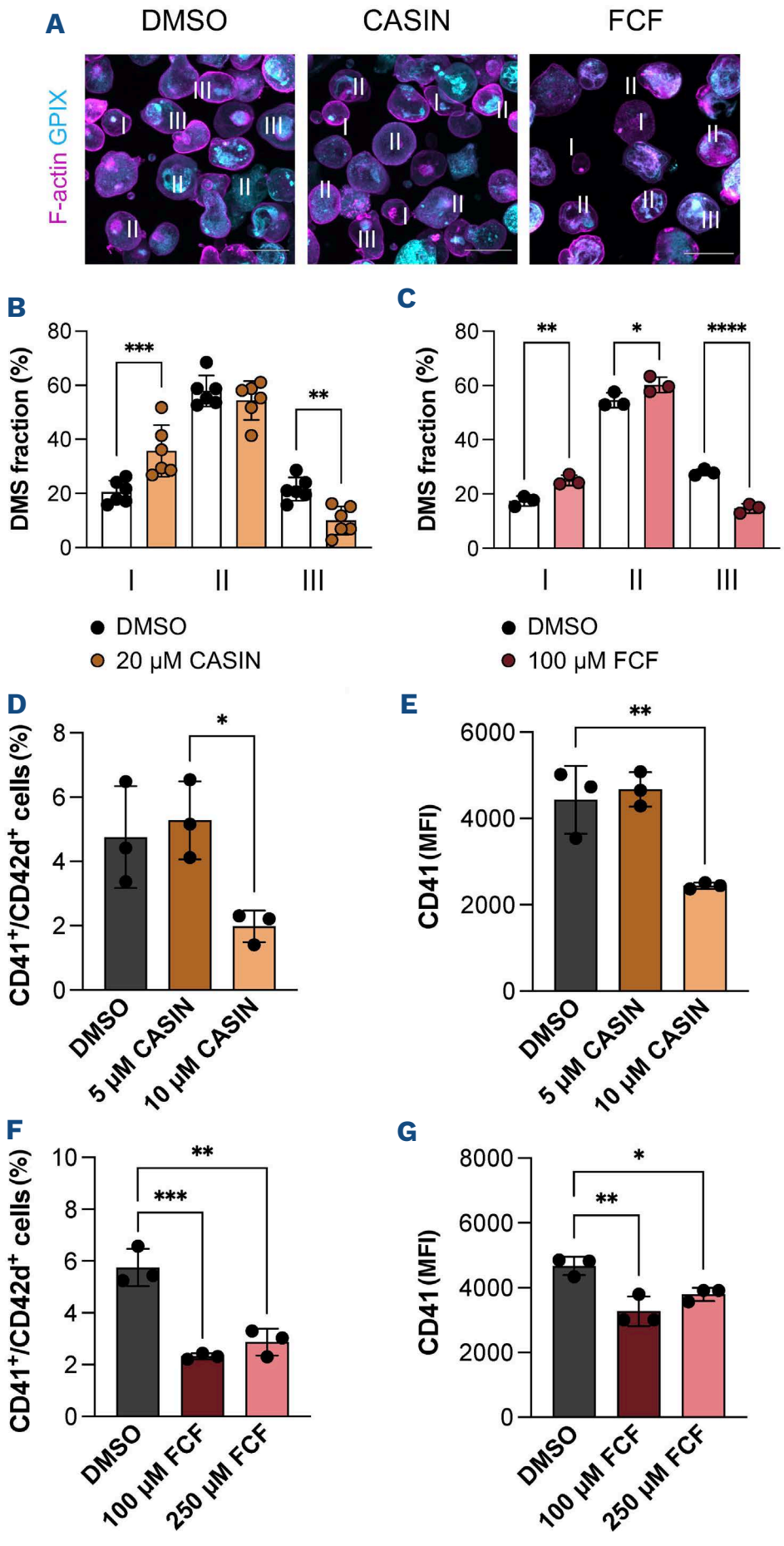

Figure 2. Cdc42 and septins are essential during megakaryocyte maturation. (A) Mature megakaryocytes (MK) were cultured in the presence of 20 µM CASIN or 100 µM forchlorfenuron (FCF) for 24 hours (hrs) and stained for filamentous (F)-actin and GPIX in solution. Stages of demarcation membrane system (DMS) maturation (I, II and III) are labeled. Scale bars: 30 µm. (B and C) Polarization of the DMS upon treatment with CASIN or FCF was manually quantified using ImageJ. Data presented as mean ± standard deviation (SD). Multiple Student *t* tests. (D and E) Percentage of CD41/CD42d-positive cells (D) and CD41 MFI (E) in DMSO and CASIN-treated bone marrow-derived MK was assessed by flow cytometry after 4 days of culture. Data presented as mean ± SD. One-way ANOVA with Sidak correction for multiple comparisons. (F and G) Percentage of CD41/CD42d-positive cells (F) and CD41 MFI (G) in DMSO and FCF-treated bone marrow-derived MK was assessed by flow cytometry after 4 days of culture. Data presented as mean ± SD. One-way ANOVA with Sidak correction for multiple comparisons. **P*<0.05; ***P*<0.01; ****P*<0.001; *****P*<0.0001. untr: untreated.

Cdc42/septins and formins but not Arp2/3-dependent actin nucleation regulate proplatelet formation *in vitro*

The importance of septins during MK maturation made us question whether septin inhibition would also translate into altered proplatelet formation. To this end, we treated mature fetal liver-derived MK with CASIN or FCF and assessed proplatelet formation kinetics over 24 hrs using a customized image analysis pipeline.[36] Inhibition of Cdc42 or septins resulted in a slightly reduced percentage of proplatelet-forming MK (DMSO: 22.7 ± 4.1%; CASIN: 13.4 ± 3.6%; FCF: 17.7 ± 7%) (Figure 3A, B) but most importantly, a markedly decreased proplatelet area (at 12 hrs: DMSO: 156,158 ± 50,691; CASIN: 26,117 ± 14,228; FCF: 36,801 ± 24,677) (Figure 3C). This observation suggested an important role of Cdc42 and septins in proplatelet elaboration, similar to what we observed upon inhibition of actin polymerization using LatA. Of note, like LatA treatment, inhibition of septins using FCF markedly impaired proplatelet motility as assessed by live-cell imaging (*Online Supplementary Videos S9, S10*). To support the hypothesis that septins are

involved in actin-dependent cytoskeletal rearrangements during proplatelet formation, we performed 3D-STORM on proplatelet-forming MK. Actin depolymerization by LatA led to the degradation of intracellular actin foci (*Online Supplementary Figure S1A*), while subplasmalemmal actin structures appeared more preserved. Moreover, condensed septin spots appeared to localize to specific subregions close to the concentrated F-actin clusters in DMSO-treated samples, whereas septins appeared highly dispersed upon depolymerization of actin foci using LatA (*Online Supplementary Figure S1B, C*).

Previous studies have suggested that actin branching might serve the diverging of proplatelets;[13] however, definitive proof for this hypothesis has been lacking. Actin nucleation, the formation of a new actin filament out of actin monomers, can be executed by several actin-binding proteins such as the protein complex Arp2/3 or the protein class of formins, some of which are downstream effectors of Cdc42.[42] However, although Arp2- and WASp-deficient mice present with microthrombocytopenia,[19,43] proplatelet formation from Arp2-deficient MK *in vitro* is unaltered,[19] while mice lacking certain formins present with impaired proplatelet formation *in vitro* similar to Cdc42-deficient mice.[44] We utilized the Arp2/3 inhibitor CK666 and analyzed proplatelet formation to assess whether Arp2/3-dependent actin branching promoted proplatelet elaboration, but did not observe any difference (Figure 3D). However, consistent with the previously described role of Arp2/3 in DMS maturation,[13] late MK maturation was impaired upon treatment of HSPC with 50 μM CK666, while CD41 MFI was unaltered (Figure 3E, F). Proplatelet-forming MK on the other hand appeared as elaborate as control MK (Figure 3G), with a similar number of proplatelet tips (Figure 3H) suggesting proplatelet formation was unaffected. Most importantly, and in line with *in vivo* findings of reduced platelet size,[19] proplatelet tip size was significantly reduced upon CK666 treatment (Figure 3 I), suggesting that Arp2/3-dependent actin nucleation and branching is dispensable for proplatelet elaboration, but important for platelet sizing. This supports observations from previous studies suggesting that Arp2/3-mediated actin nucleation and branching are important for the formation of sheet-like actin protrusions, i.e., during lamellipodia formation,[19] but are dispensable for linear actin elongation and elaboration such as required for proplatelet formation. In contrast, formin inhibition using the small molecule inhibitor of formin homology 2 domains

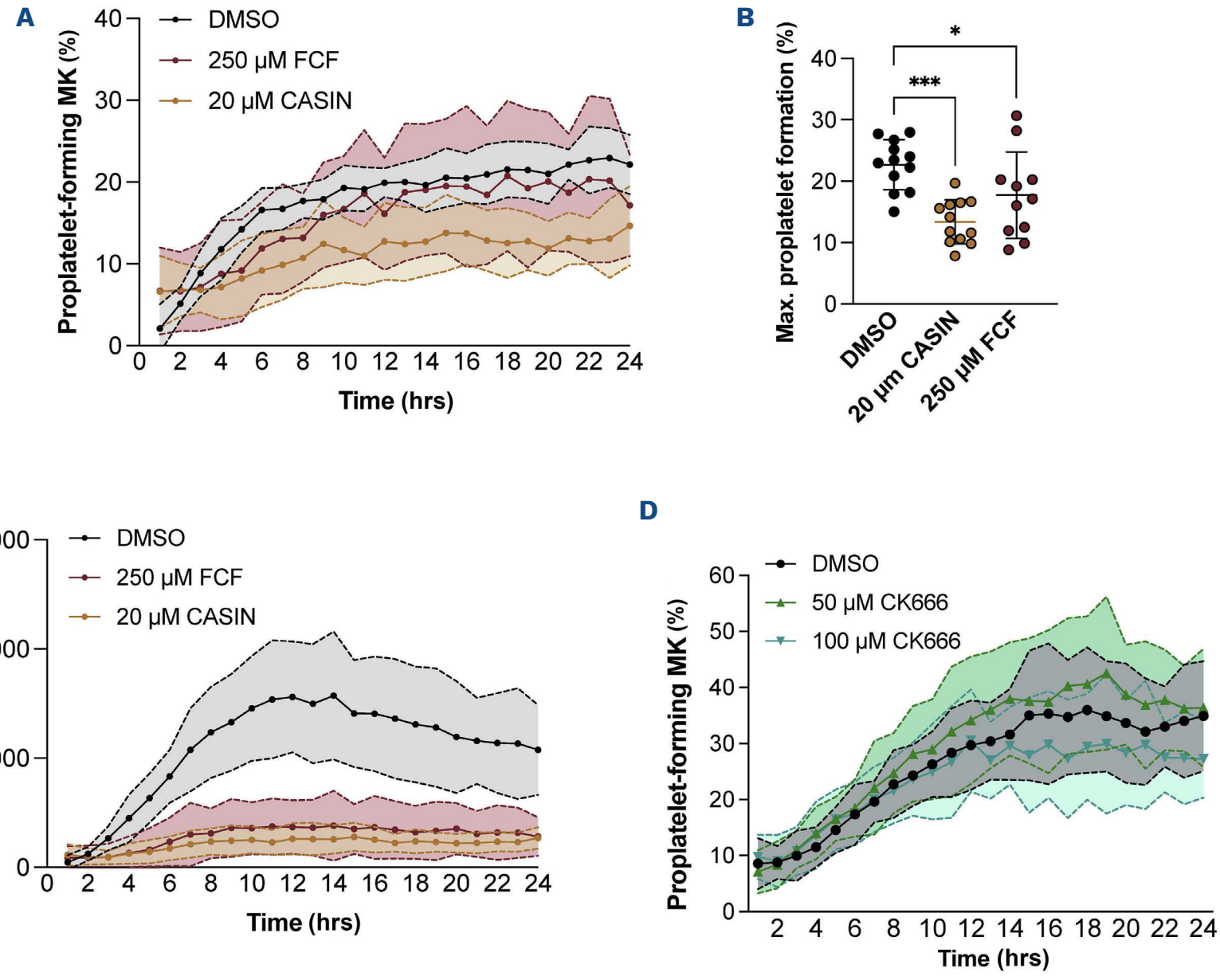

Continued on following page.

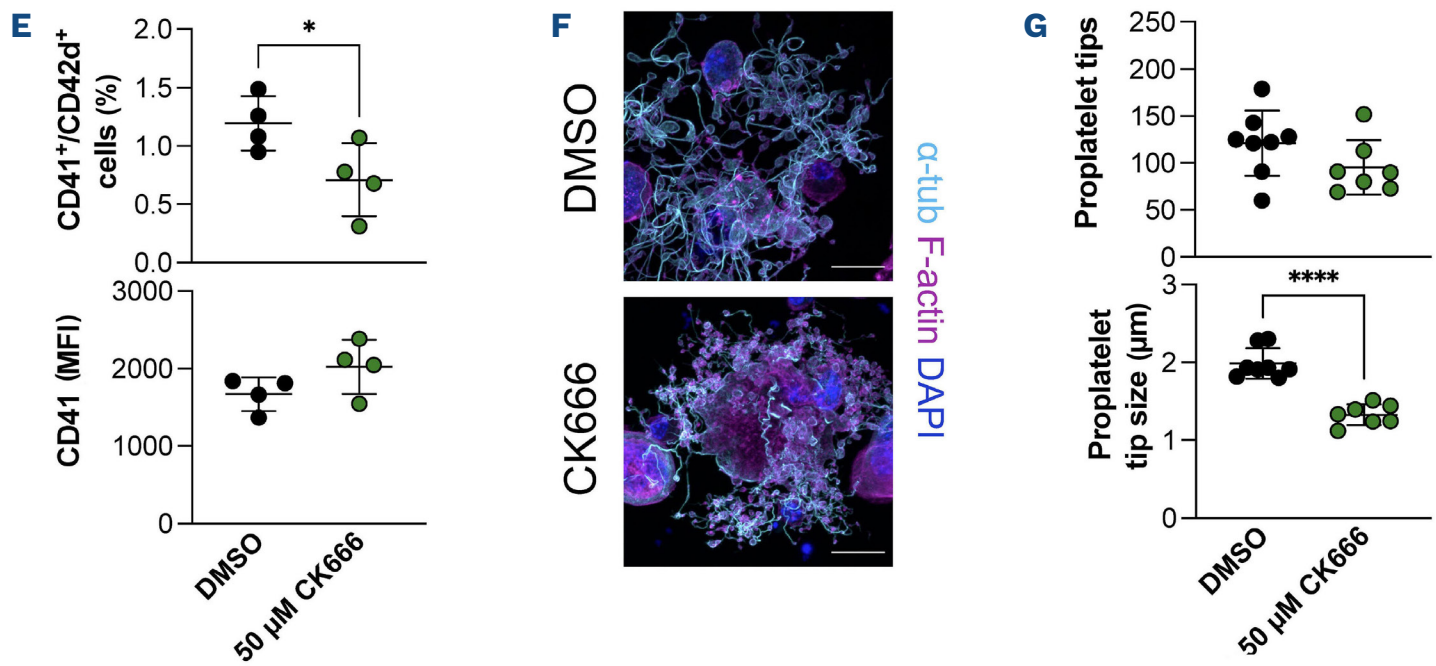

Figure 3. Proplatelet elaboration is dependent on Cdc42/septins/formins but not Arp2/3. (A-C) Fetal liver-derived megakaryocytes (MK) were treated with the indicated concentrations of CASIN, forchlorfenuron (FCF), or vehicle control (DMSO) and imaged every hour for 24 hours (hrs) using an Incucyte imaging system. Percentage of (A and B) proplatelet-forming fetal liver-derived MK and (C) proplatelet area were analyzed using a custom imaging pipeline. N=3 mice. There were 3 technical repeats. Data presented as mean ± standard deviation (SD). One-way ANOVA with Sidak correction for multiple comparisons. (D) Fetal liver-derived MK were treated with the indicated concentrations of the Arp2/3 inhibitor CK666 and imaged for 24 hrs using an Incucyte imaging system. N=3 mice. There were 3 technical repeats. Data presented as mean ± SD. Percentage of (E) CD41/CD42d-positive cells and (F) CD41 mean fluorescence intensity (MFI) in DMSO and CK666-treated bone marrow-derived MK was assessed by flow cytometry after 4 days of culture. Data presented as mean ± SD. Unpaired, two-tailed Student *t* test. (G) Visualization and (H and I) quantification of proplatelet tip number and size in DMSO- and CK666-treated bone marrow-derived MK. Data presented as mean ± SD. Unpaired, two-tailed Student *t* test. *P<0.05; ***P<0.001; ****P<0.0001.

(SMIFH2) dose-dependently reduced the percentage of proplatelet-forming MK (*Online Supplementary Figure S2A, B*). Moreover, proplatelet area was significantly reduced (*Online Supplementary Figure S2C*), similar to Cdc42/septin inhibition. These findings imply that an Arp2/3-independent actin nucleation pathway involving formins accounts for proplatelet elaboration and movement.

Defective F-actin dynamics underlie reduced proplatelet area upon Cdc42/septin/formin inhibition

Our previous data suggest that Cdc42/septin inhibition interfered with proplatelet elaboration by affecting actin dynamics (Figure 3C). To verify this, we performed immunofluorescence staining for F-actin and α-tubulin on proplatelet-forming MK treated with either 20 µM CASIN or 100 µM FCF (*Online Supplementary Figure S2D*). Consistent with our kinetic analysis, we found a reduced number of proplatelet tips and an increased tip diameter in MK upon inhibition of Cdc42 or septins (*Online Supplementary Figure SE, F*). To investigate how septin inhibition affected actin dynamics during proplatelet formation, we quantified actin-rich nodules in proplatelet-forming MK upon FCF treatment (100 µM). While actin nodules were visible in DMSO-treated MK, FCF-treatment attenuated actin rearrangements, resulting in 'empty' proplatelet tips (*Online Supplementary Figure SG, H*), while cortical F-actin structures were preserved. MK stained live with SiR-Actin displayed actin-rich dots and proplatelet were highly motile (*Online Supplementary Video S11*), which was abrogated upon treatment with either LatA (*Online Supplementary Video S12*) or FCF (*Online Supplementary Video S13*).

Since FCF is a universal septin inhibitor, we next aimed to assess how FCF treatment affected the localization of individual septins (2, 5, 7 and 9) in bone marrow-derived proplatelet-forming MK. While Sept5 predominantly localized to the actin cytoskeleton, Sept2 and 7 localized to both microtubules and F-actin, and Sept9 exclusively localized to microtubules (Figure 4A-D), which was quantified using Costes Pearson coefficients for either F-actin or α-tubulin (Figure 4E, F). While colocalization of Sept5 and 7 with cortical actin structures was preserved (or even enhanced) upon FCF treatment, despite a general decrease in intracellular actin foci as shown above, septin 2, 7 and 9 colocalization to microtubules was disturbed as shown in line plots (Figure 5A-D). Similar differences in staining patterns upon FCF-treatment were observed in murine fetal liver-derived MK (*Online Supplementary Figure S3A-F*). As previously described in platelets,[30] septins that associated with microtubules (2 and 9) formed ring-like structures, which were even more abundant upon treatment of MK with 100 µM FCF (Figure 5E-G), a phenomenon previously also described in fibroblasts treated with CytoD.[45] To further investigate the intracellular localization of septins upon cytoskeletal rearrangements, bone marrow-derived MK were allowed to spread on a fibrinogen-coated surface and were imaged by confocal microscopy. Like proplate-

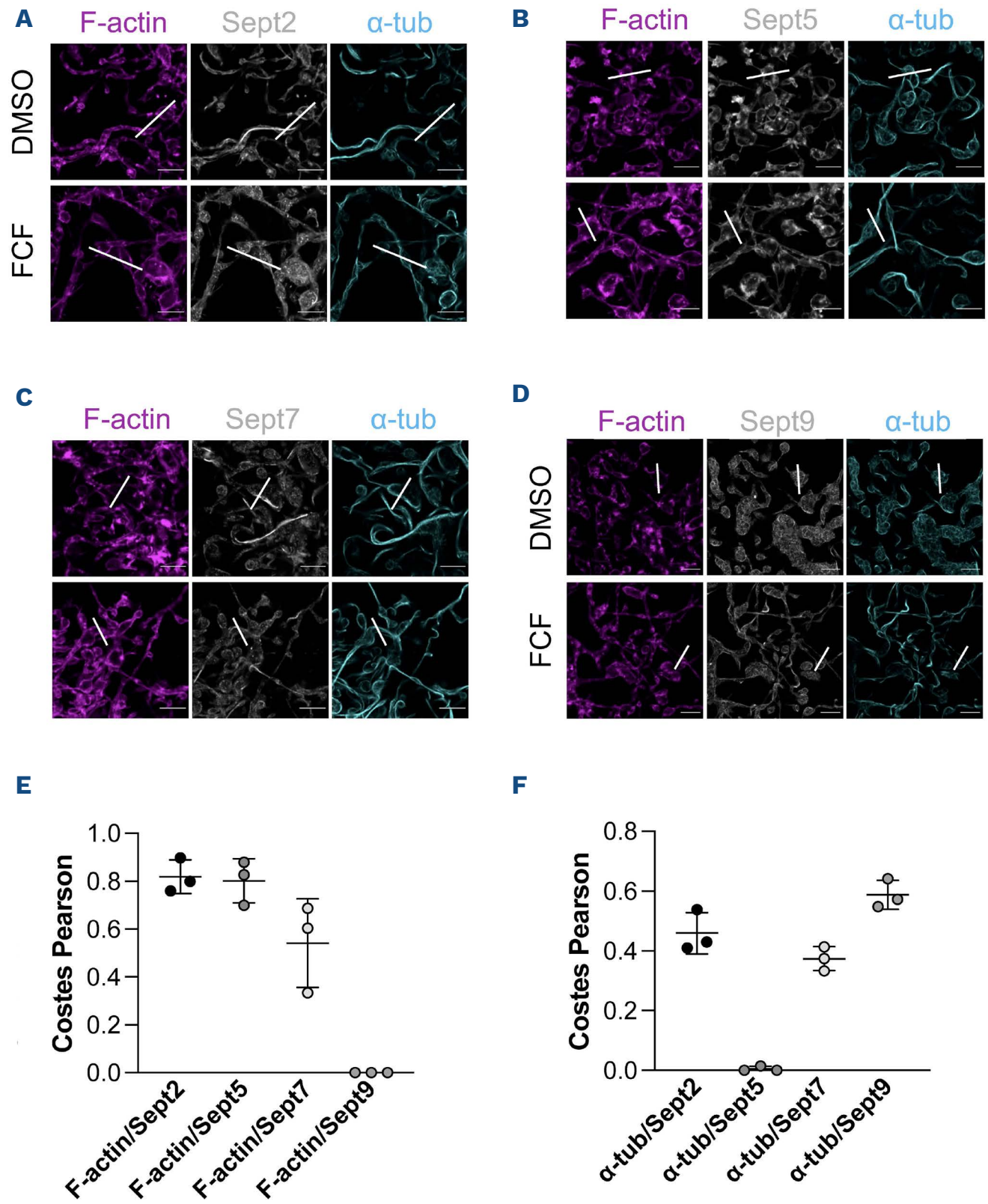

Figure 4. Distinct localization of different septin classes to F-actin or microtubules. (A-D) Visualization of filamentous (F)-actin, α-tubulin and (A) Sept2, (B) Sept5, (C) Sept7 and (D) Sept9 in bone marrow-derived proplatelet-forming megakaryocytes (MK) upon DMSO or forchlorfenuron (FCF) treatment. Scale bars: 15 μm; insets: 5 μm. Line plots connected to white lines are shown in Figure 5. Co-localization analysis for (E) F-actin/septins and (F) α-tubulin/septins was performed in proplatelet-forming MK. Data presented as mean ± standard deviation. One dot represents one representative cell imaged with super-resolution microscopy at a Zeiss LSM880 (63x; Airyscan module). Costes Pearson: Costes Pearson coefficients.

let-forming MK, Sept2 localized to both microtubules and actin fibers, while Sept5 almost exclusively concentrated to actin structures (*Online Supplementary Figure S4A-D*). In contrast, while Sept7 appeared to associate more closely to microtubules, Sept9 exclusively localized to microtubules (*Online Supplementary Figure S4E-H*). In summary, our data reveal that different septins associate with microtubule and F-actin structures, suggesting that they might be capable of bridging forces between the two cytoskeletal compartments.

F-actin/septin forces enhance proplatelet formation under stress

While we show that a Cdc42/septin/F-actin axis is important for proplatelet formation dynamics *in vitro*, we next wanted to assess the relevance of this machinery *in vivo*. To investigate how enhanced megakaryocyte activity due to synchronized thrombopoiesis affected the expression of cytoskeletal proteins, we utilized a model of antibody-induced platelet depletion.[46] We visualized the actin and microtubule cytoskeleton in femoral cryosections days

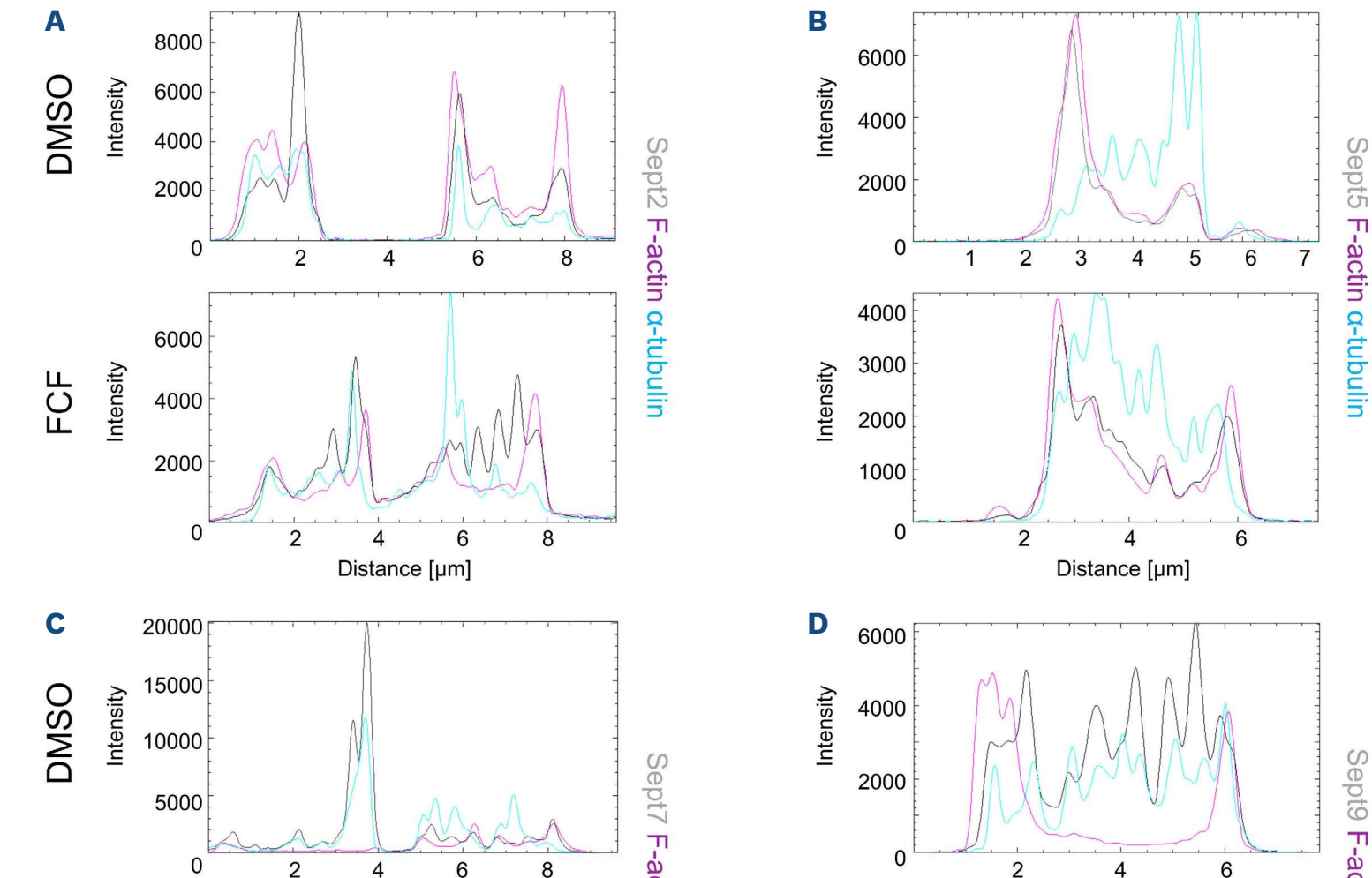

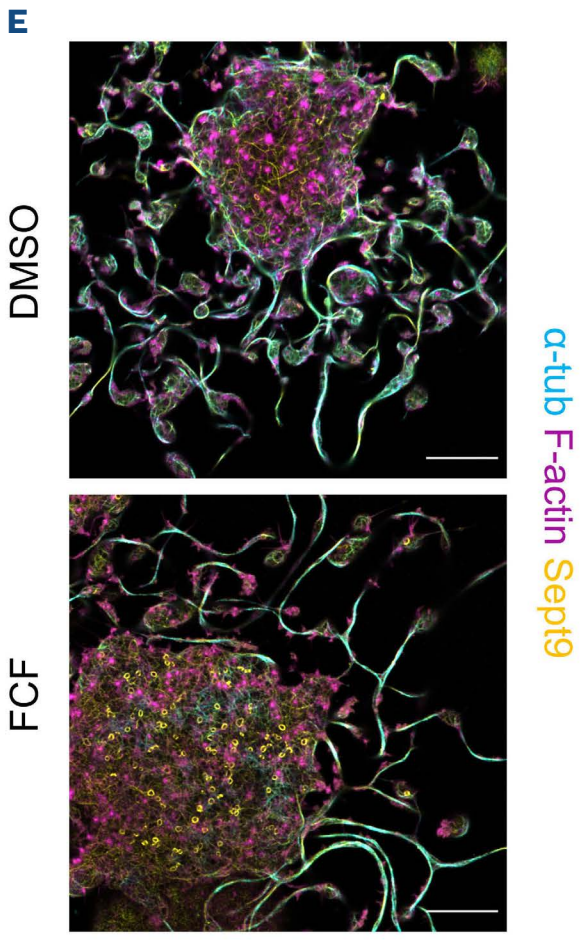

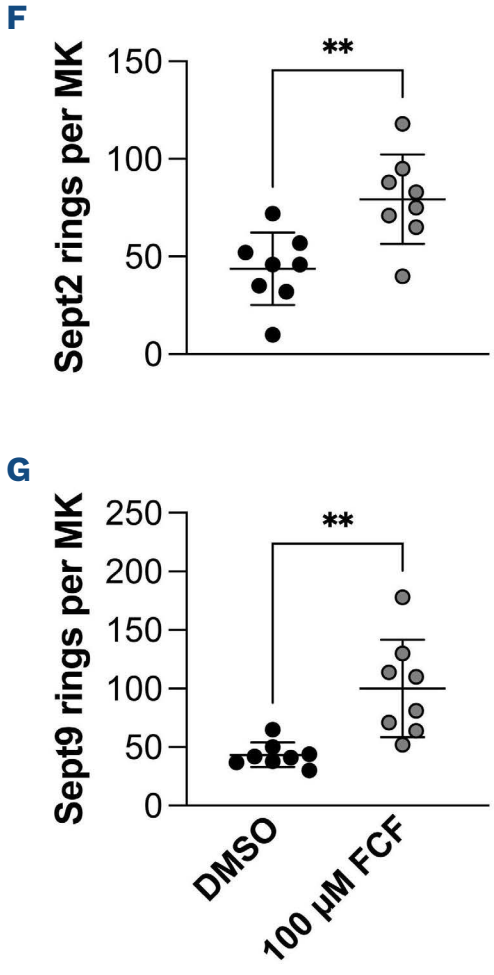

Figure 5. Disruption of septin localization upon septin inhibition. (A-D) Line plots for filamentous (F)-actin, α-tubulin and (A) Sept2, (B) Sept5, (C) Sept7 and (D) Sept9 in bone marrow-derived proplatelet-forming megakaryocytes (MK) upon DMSO or forchlorfenuron (FCF) treatment. (E-G) Septin ring formation in proplatelet-forming MK was (E) visualized and (F and G) quantified in DMSO- and FCF-treated cells. Data presented as mean ± standard deviation. N=2. Unpaired, two-tailed Student *t* test. ***P*<0.01. One dot represents one cell.

(144 hrs) after platelet depletion (*Online Supplementary Figure S5A*), when platelet counts began to recover. The significant rise in platelet counts at that timepoint suggests that MK are actively generating platelets at a higher rate, as suggested by other studies.[47] Of note, the number of MK was described to be unaltered in platelet-depleted mice.[48] F-actin appeared to specifically localize to a cortical ring surrounding the DMS, a phenomenon that was even more apparent in MK derived from platelet-depleted mice, which exhibited a highly increased expression of F-actin overall (Figure 6A, B). In contrast, expression of β1-tubulin was comparable to the control (*Online Supplementary Figure S5B, C*). To investigate whether the expression of different septins was also subject to these changes upon enforced platelet generation we stained cryosections for Sept2, 5, 7 and 9. While Sept2 expression was comparable to the control (Figure 6C, D), similar to what we observed for β1-tubulin, we found a marked increase in Sept5 (Figure 6E, F), Sept7 (Figure 6G, H) and Sept9 expression (Figure 6 I, J) upon platelet depletion, suggesting that a palindromic oligomer consisting of these septins might be subject to changes upon challenge. To verify our *in vitro* observa-

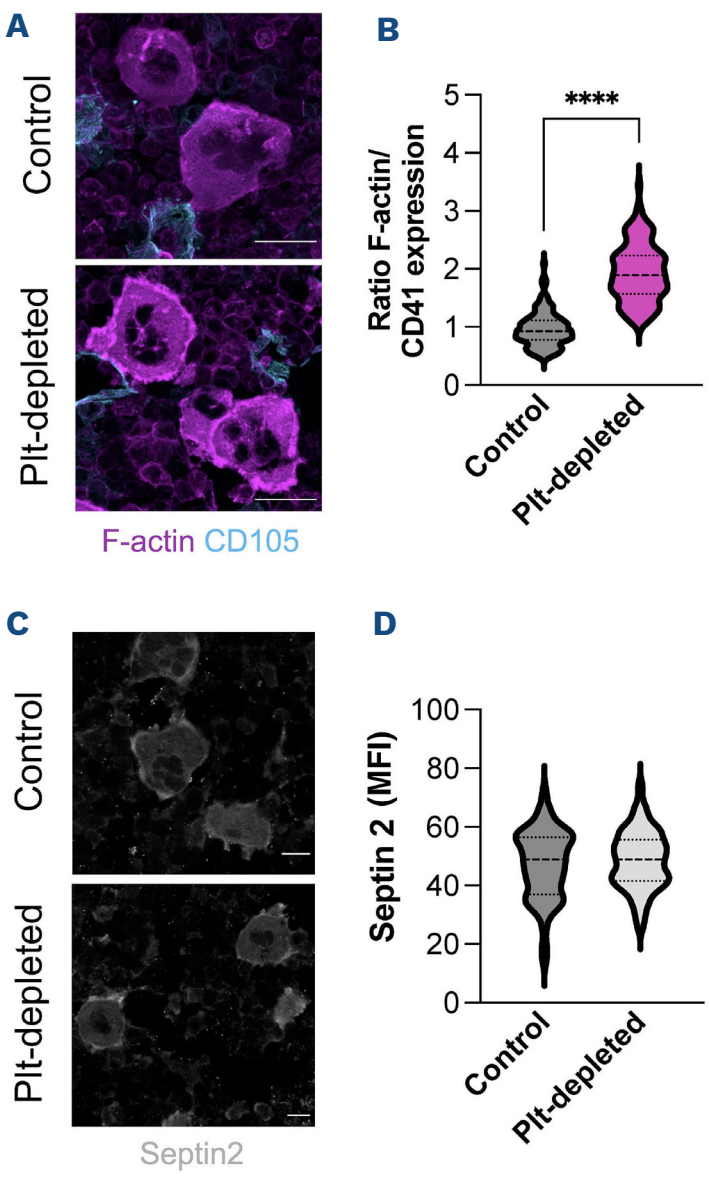

Figure 6. Enhanced thrombopoiesis increases (F)-actin and septin expression *in situ*. (A and B) Mean fluorescence intensity (MFI) of filamentous (F)-actin was visualized and quantified in femoral cryosections derived from control and platelet (Plt)-depleted mice. N=4 mice. At least 50 cells were counted per group. Data presented as mean ± standard deviation (SD). Unpaired, two-tailed Student *t* test. (C-J) Mean fluorescence intensity (MFI) of (C and D) Sept2, (E and F) Sept5, (G and H) Sept7, and (I and J) Sept9 was visualized and quantified in femoral cryosections derived from control and platelet-depleted mice. N=3 mice. Three independent experiments. At least 40 cells were counted per mice. Data presented as mean ± SD. Unpaired, two-tailed Student *t* test. ***P*<0.01; *****P*<0.0001.

tions, we performed colocalization analysis for F-actin and found the lowest association with Sept2 and Sept9 (*Online Supplementary Figure S5D*), comparable to what we observed in proplatelet-forming MK. In summary, our findings identify a novel and key role for septins in bridging intracellular actin-microtubule crosstalk in MK, inhibition of which impairs proplatelet formation.

Discussion

How the F-actin cytoskeleton regulates proplatelet formation has been puzzling researchers for decades, since inhibition of actin polymerization has been proposed to both inhibit,[14,15] as well as to induce, proplatelet formation.[16,17] Although a variety of publications have suggested that F-actin dynamics are important during proplatelet formation, the underlying mechanisms have never fully been elucidated. This is partly due to the use of knockout mice, which, in addition to impaired proplatelet formation, usually also exhibit defective MK maturation due to the important role of F-actin in DMS development. By performing live-cell imaging on proplatelet-forming MK, we observed that proplatelet formation was initiated earlier upon inhibition of actin polymerization; however, this early increase later evolved into highly defective proplatelet bead formation and elaboration, resulting in the appearance of stringy, unbeaded proplatelets (Figure 1B-D). We show that a similarly defective proplatelet elaboration can be observed upon inhibition of Cdc42 or the cytoskeletal class of septins. The defects were instigated by impaired intracellular F-actin dynamics, while the cortical actin cytoskeleton and microtubule sliding appeared to be unaffected, suggesting intracellular F-actin to account for proplatelet elaboration (i.e., the formation of elaborate proplatelet beads).

An early study by Kinoshita *et al*. elegantly demonstrated that inhibition of actin polymerization using CytoD promotes septin ring formation, since septin filaments dissociated from actin fibers.[45] Inhibition of septins using siRNA in turn attenuated intracellular actin filament assembly, while cortical actin and septin structures were mostly unaffected. Our data support these findings and reveal that inhibition of septins similarly induced their dissociation from F-actin or microtubule fibers, thus enhancing septin ring formation in the MK cell body or association with the cortical F-actin cytoskeleton (Figure 5E-G), while promoting aberrant intracellular actin dynamics. This was in line with our observations upon treatment of MK with LatA (*Online Supplementary Figure S1A*), where cortical F-actin structures were mostly retained. In addition to the preservation of cortical actin and septin structures, LatA treatment only marginally affected microtubule sliding (Figure 1J), which thus appears to be important for the elongation of proplatelet shafts, while intracellular cytoskeletal dynamics are required for the development and movement of proplatelet beads. The formation of septin rings upon septin inhibition was restricted to the microtubule-binding septins 2, 7 and 9. However, previous studies have found different septin classes to form palindromic oligomers,[49,50] suggesting that inhibition of one class will inadvertently affect the expression and function of its associated septins. This connection may thus explain the effects on intracellular actin dynamics observed upon septin inhibition. Sept5 was previously shown to associate with Sept7 and 9,[30] whose expression was markedly altered upon FCF treatment. At the same time, our *in vivo* data revealed that

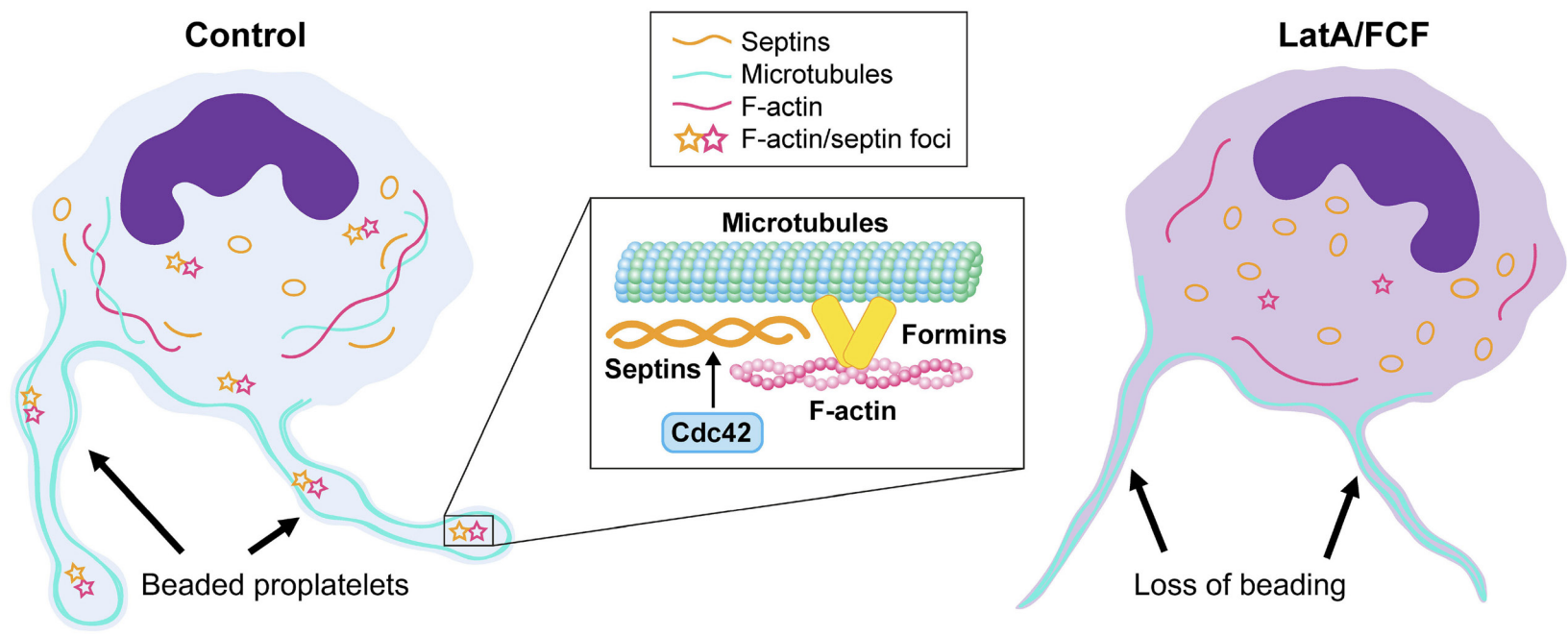

Figure 7. A Cdc42/septin axis regulates F-actin dynamics during proplatelet formation. In control megakaryocytes (MK), intracellular filamentous (F)-actin (magenta) integrates with septins (yellow) and microtubules (cyan). F-actin/septin-rich nodules within proplatelet beads interact with formin proteins and promote proplatelet beading. Arrows point towards proplatelet beads along the proplatelet shaft. Treatment with actin polymerization inhibitors (LatA) or the septin inhibitor forchlorfenuron (FCF) increases septin dispersion/ring formation and impairs transduction of F-actin forces to the elongating proplatelet.

only the expression of these septins is subject to changes in a model of enhanced thrombopoiesis (Figure 6), which indicates that septin oligomers *in vivo* might consist of a specific array of septins.

In addition to the effects observed on proplatelet formation, septin inhibition also affected MK maturation (Figure 2F, G), which might be attributed to an impaired development of the DMS due to interference with the actin cytoskeleton. However, it might also be explained by the high concentration of FCF generally used *in vitro*, which could elicit off-target effects on a variety of signaling pathways, as previously suggested.[51] Moreover, septins play an essential role in cytokinesis in both yeast as well as mammals,[52] which might affect polyploidization. This is in line with a previous study revealing defective endomitosis in MK lacking PAK2, another downstream target of Cdc42.[22] Ultimately, only genetic strategies using a CRISPR-approach or Pf4-Cre-mediated gene deletions will answer how septins regulate MK maturation.

A variety of previous studies have described the importance of Cdc42 in MK and platelets.[15,21,39] However, while it was shown that the impaired maturation and proplatelet formation observed upon Cdc42 inhibition partially resulted from altered neural WASp (n-WASp) activity,[53] we demonstrate that both are also instigated by inhibitory effects on septin polymerization. Strikingly, this impairment in proplatelet formation occurred independent of the Arp2/3 since inhibition of Arp2/3 did not reduce proplatelet formation *in vitro* (Figure 3D). Platelets derived from Arp2/3- and WASp-deficient mice exhibit an enhanced stability of the cortical microtubule ring,[19,54] while microtubule sliding and cortical microtubule bundles were unaffected by either Cdc42 or septin inhibition. Our findings are more reminiscent of an actin network found in neurons, in which intracellular actin foci occurred independent of the cortical actin cytoskeleton,[38] similar to what we observed in MK (*Online Supplementary Video S10*), and were formed independent of Arp2/3.[34] This neuronal actin network was subject to formin proteins, inhibition of which severely compromised proplatelet formation as well (*Online Supplementary Figure S2A-C*). More evidence for this occurring independent of the Arp2/3/WASp pathways comes from the observation that treatment of platelets with a formin inhibitor retained the cortical microtubule ring, while the actin cytoskeleton was highly disrupted.[55] The data thus imply that an intracellular cytoskeletal network consisting of F-actin, formins and septins is responsible for the transduction of forces, which are essential for the formation of beads along the proplatelet shaft (Figure 7).

In summary, our data reveal that septins in MK distinctly associate with the intracellular actin and microtubule cytoskeleton. Inhibition of either septins, formins or their upstream regulator Cdc42 resulted in disrupted F-actin dynamics leading to impaired proplatelet elaboration, as observed upon inhibition of actin polymerization. These data unravel an important role of an intracellular cytoskeletal network in MK and identify a previously unknown role for septins in MK biology.

Disclosures

JEI has financial interest in and is a founder of StellularBio, a biotechnology company focused on making donor-independent platelet-like cells at scale. The interests of JEI are managed by Boston Children's Hospital. All other authors have no conflicts of interest to disclose.

Contributions

ICB, ARW and JEI are responsible for the study concept. ICB, ARW, BAU, ARS, FF and IT are responsible for the methodology and investigation. JEI supervised the study. ICB and ARW wrote the original draft of the manuscript. ICB, ARW, KX, KRM and JEI are responsible for writing, reviewing and editing the manuscript for publication.

Acknowledgments

We thank Emma Nikols, Daniela Freire, Clementine Payne and Karen Guo for excellent technical assistance as well as Harvey Roweth for proofreading the manuscript. We thank Kristin Johnson for generating the graphical abstract.

Funding

ARW was supported by an F32 postdoctoral fellowship (1F32HL152486-01). ICB is supported by a Walter Benjamin Fellowship of the German Research Foundation (DFG; BE 7766/2-1). JEI is supported by the National Institute of Health National Heart, Lung and Blood Institute (R01HL68130 and R35HL161175).

Data-sharing statement

All data are available upon request from the corresponding author.

References

1. Italiano JE Jr, Lecine P, Shivdasani RA, Hartwig JH. Blood platelets are assembled principally at the ends of proplatelet processes produced by differentiated megakaryocytes. J Cell Biol. 1999;147(6):1299-1312.
2. Eckly A, Scandola C, Oprescu A, et al. Megakaryocytes use in vivo podosome-like structures working collectively to penetrate the endothelial barrier of bone marrow sinusoids. J Thromb Haemost. 2020;18(11):2987-3001.
3. Schachtner H, Calaminus SD, Sinclair A, et al. Megakaryocytes assemble podosomes that degrade matrix and protrude through basement membrane. Blood. 2013;121(13):2542-2552.
4. Italiano JE Jr, Patel-Hett S, Hartwig JH. Mechanics of

proplatelet elaboration. J Thromb Haemost. 2007;5(Suppl 1):18-23.
5. Thon JN, Montalvo A, Patel-Hett S, et al. Cytoskeletal mechanics of proplatelet maturation and platelet release. J Cell Biol. 2010;191(4):861-874.
6. Bennett C, Lawrence M, Guerrero JA, et al. CRLF3 plays a key role in the final stage of platelet genesis and is a potential therapeutic target for thrombocythemia. Blood. 2022;139(14):2227-2239.
7. Bender M, Thon JN, Ehrlicher AJ, et al. Microtubule sliding drives proplatelet elongation and is dependent on cytoplasmic dynein. Blood. 2015;125(5):860-868.
8. Richardson JL, Shivdasani RA, Boers C, Hartwig JH, Italiano JE Jr. Mechanisms of organelle transport and capture along proplatelets during platelet production. Blood. 2005;106(13):4066-4075.
9. Khan AO, Slater A, Maclachlan A, et al. Post-translational polymodification of beta1-tubulin regulates motor protein localisation in platelet production and function. Haematologica. 2022;107(1):243-259.
10. Strassel C, Magiera MM, Dupuis A, et al. An essential role for alpha4A-tubulin in platelet biogenesis. Life Sci Alliance. 2019;2(1):e201900309.
11. Mbiandjeu S, Balduini A, Malara A. Megakaryocyte cytoskeletal proteins in platelet biogenesis and diseases. Thromb Haemost. 2022;122(5):666-678.
12. Eckly A, Heijnen H, Pertuy F, et al. Biogenesis of the demarcation membrane system (DMS) in megakaryocytes. Blood. 2014;123(6):921-930.
13. Schulze H, Korpal M, Hurov J, et al. Characterization of the megakaryocyte demarcation membrane system and its role in thrombopoiesis. Blood. 2006;107(10):3868-3875.
14. Rojnuckarin P, Kaushansky K. Actin reorganization and proplatelet formation in murine megakaryocytes: the role of protein kinase calpha. Blood. 2001;97(1):154-161.
15. Antkowiak A, Viaud J, Severin S, et al. Cdc42-dependent F-actin dynamics drive structuration of the demarcation membrane system in megakaryocytes. J Thromb Haemost. 2016;14(6):1268-1284.
16. Tablin F, Castro M, Leven RM. Blood platelet formation in vitro. The role of the cytoskeleton in megakaryocyte fragmentation. J Cell Sci. 1990;97(Pt 1):59-70.
17. Avanzi MP, Izak M, Oluwadara OE, Mitchell WB. Actin inhibition increases megakaryocyte proplatelet formation through an apoptosis-dependent mechanism. PLoS One. 2015;10(4):e0125057.
18. Rohatgi R, Ma L, Miki H, et al. The interaction between N-WASP and the Arp2/3 complex links Cdc42-dependent signals to actin assembly. Cell. 1999;97(2):221-231.
19. Paul DS, Casari C, Wu C, et al. Deletion of the Arp2/3 complex in megakaryocytes leads to microthrombocytopenia in mice. Blood Adv. 2017;1(18):1398-1408.
20. Haddad E, Cramer E, Riviere C, et al. The thrombocytopenia of Wiskott Aldrich syndrome is not related to a defect in proplatelet formation. Blood. 1999;94(2):509-518.
21. Heib T, Hermanns HM, Manukjan G, et al. RhoA/Cdc42 signaling drives cytoplasmic maturation but not endomitosis in megakaryocytes. Cell Rep. 2021;35(6):109102.
22. Kosoff RE, Aslan JE, Kostyak JC, et al. Pak2 restrains endomitosis during megakaryopoiesis and alters cytoskeleton organization. Blood. 2015;125(19):2995-3005.
23. Nakos K, Alam MNA, Radler MR, et al. Septins mediate a microtubule-actin crosstalk that enables actin growth on microtubules. Proc Natl Acad Sci U S A. 2022;119(50):e2202803119.
24. Salameh J, Cantaloube I, Benoit B, Pous C, Baillet A. Cdc42 and its BORG2 and BORG3 effectors control the subcellular localization of septins between actin stress fibers and microtubules. Curr Biol. 2021;31(18):4088-4103.
25. Spiliotis ET, Nakos K. Cellular functions of actin- and microtubule-associated septins. Curr Biol. 2021;31(10):R651-R666.
26. Hall PA, Jung K, Hillan KJ, Russell SE. Expression profiling the human septin gene family. J Pathol. 2005;206(3):269-278.
27. Neubauer K, Zieger B. The mammalian septin interactome. Front Cell Dev Biol. 2017;5:3.
28. Kim OV, Litvinov RI, Mordakhanova ER, Bi E, Vagin O, Weisel JW. Contribution of septins to human platelet structure and function. iScience. 2022;25(7):104654.
29. Blaser S, Horn J, Wurmell P, et al. The novel human platelet septin SEPT8 is an interaction partner of SEPT4. Thromb Haemost. 2004;91(5):959-966.
30. Martinez C, Corral J, Dent JA, Sesma L, Vicente V, Ware J. Platelet septin complexes form rings and associate with the microtubular network. J Thromb Haemost. 2006;4(6):1388-1395.
31. Dent J, Kato K, Peng XR, et al. A prototypic platelet septin and its participation in secretion. Proc Natl Acad Sci U S A. 2002;99(5):3064-3069.
32. Iwase M, Okada S, Oguchi T, Toh-e A. Forchlorfenuron, a phenylurea cytokinin, disturbs septin organization in Saccharomyces cerevisiae. Genes Genet Syst. 2004;79(4):199-206.
33. Neubauer K, Jurk K, Petermann V, Kumm E, Zieger B. Impaired platelet function in Sept8-deficient mice in vitro. Thromb Haemost. 2021;121(4):484-494.
34. Ganguly A, Tang Y, Wang L, et al. A dynamic formin-dependent deep F-actin network in axons. J Cell Biol. 2015;210(3):401-417.
35. Zuidscherwoude M, Green HLH, Thomas SG. Formin proteins in megakaryocytes and platelets: regulation of actin and microtubule dynamics. Platelets. 2019;30(1):23-30.
36. French SL, Vijey P, Karhohs KW, et al. High-content, label-free analysis of proplatelet production from megakaryocytes. J Thromb Haemost. 2020;18(10):2701-2711.
37. Thon JN, Mazutis L, Wu S, et al. Platelet bioreactor-on-a-chip. Blood. 2014;124(12):1857-1867.
38. Xu K, Zhong G, Zhuang X. Actin, spectrin, and associated proteins form a periodic cytoskeletal structure in axons. Science. 2013;339(6118):452-456.
39. Pleines I, Dutting S, Cherpokova D, et al. Defective tubulin organization and proplatelet formation in murine megakaryocytes lacking Rac1 and Cdc42. Blood. 2013;122(18):3178-3187.
40. Versele M, Thorner J. Septin collar formation in budding yeast requires GTP binding and direct phosphorylation by the PAK, Cla4. J Cell Biol. 2004;164(5):701-715.
41. Spindler M, van Eeuwijk JMM, Schurr Y, et al. ADAP deficiency impairs megakaryocyte polarization with ectopic proplatelet release and causes microthrombocytopenia. Blood. 2018;132(6):635-646.
42. Firat-Karalar EN, Welch MD. New mechanisms and functions of actin nucleation. Curr Opin Cell Biol. 2011;23(1):4-13.
43. Sabri S, Foudi A, Boukour S, et al. Deficiency in the Wiskott-Aldrich protein induces premature proplatelet formation and platelet production in the bone marrow compartment. Blood. 2006;108(1):134-140.
44. Stritt S, Nurden P, Turro E, et al. A gain-of-function variant in

DIAPH1 causes dominant macrothrombocytopenia and hearing loss. Blood. 2016;127(23):2903-2914.
45. Kinoshita M, Field CM, Coughlin ML, Straight AF, Mitchison TJ. Self- and actin-templated assembly of mammalian septins. Dev Cell. 2002;3(6):791-802.
46. Nieswandt B, Bergmeier W, Rackebrandt K, Gessner JE, Zirngibl H. Identification of critical antigen-specific mechanisms in the development of immune thrombocytopenic purpura in mice. Blood. 2000;96(7):2520-2527.
47. Heazlewood SY, Ahmad T, Cao B, et al. High ploidy large cytoplasmic megakaryocytes are hematopoietic stem cells regulators and essential for platelet production. Nat Commun. 2023;14(1):2099.
48. Stegner D, van Eeuwijk JMM, Angay O, et al. Thrombopoiesis is spatially regulated by the bone marrow vasculature. Nat Commun. 2017;8(1):127.
49. Dolat L, Hunyara JL, Bowen JR, et al. Septins promote stress fiber-mediated maturation of focal adhesions and renal epithelial motility. J Cell Biol. 2014;207(2):225-235.
50. Martins CS, Taveneau C, Castro-Linares G, et al. Human septins organize as octamer-based filaments and mediate actin-membrane anchoring in cells. J Cell Biol. 2023;222(3):e202203016.
51. Heasley LR, Garcia G 3rd, McMurray MA. Off-target effects of the septin drug forchlorfenuron on nonplant eukaryotes. Eukaryot Cell. 2014;13(11):1411-1420.
52. Menon MB, Sawada A, Chaturvedi A, et al. Genetic deletion of SEPT7 reveals a cell type-specific role of septins in microtubule destabilization for the completion of cytokinesis. PLoS Genet. 2014;10(8):e1004558.
53. Palazzo A, Bluteau O, Messaoudi K, et al. The cell division control protein 42-Src family kinase-neural Wiskott-Aldrich syndrome protein pathway regulates human proplatelet formation. J Thromb Haemost. 2016;14(12):2524-2535.
54. Bender M, Stritt S, Nurden P, et al. Megakaryocyte-specific Profilin1-deficiency alters microtubule stability and causes a Wiskott-Aldrich syndrome-like platelet defect. Nat Commun. 2014;5:4746.
55. Green HLH, Zuidscherwoude M, Alenazy F, Smith CW, Bender M, Thomas SG. SMIFH2 inhibition of platelets demonstrates a critical role for formin proteins in platelet cytoskeletal dynamics. J Thromb Haemost. 2020;18(4):955-967.